

TOCHNOG PROFESSIONAL Validation manual
Version 5.3

FEAT - Finite Element Application Technology

March 15, 2010

Contents

1	Conditions	3
2	Validation calculations	4
2.1	Validation 1: Backward facing step (fluid flow)	4
2.2	Validation 2: Confined compression of fluid filled porous material	5
2.3	Validation 3: Plasticity in plate with circular hole	6
2.4	Validation 4: Two-dimensional convection and diffusion	7
2.5	Validation 7: Global mesh refinement over polynomial domain	8
2.6	Validation 10: Shear of low-tension material (cracking)	9
2.7	Validation 11: Propagation of a disturbance in the wave equation.	10
2.8	Validation 12: Contact frictional heat generation.	11
2.9	Validation 14: Continuous metal forming.	13
2.10	Validation 15: Generation of two holes in 2D mesh.	14
2.11	Validation 16: Bearing capacity of foundation.	15
2.12	Validation 17: Hertz contact problem.	16
2.13	Validation 18: Thermally induced stresses in plate.	17
2.14	Validation 19: Nonlocal plasticity in softening bar.	18
2.15	Validation 22: Constant volume cylindrical compression with Cam Clay.	20
2.16	Validation 23: Automatic local mesh refinement near shear band.	21

1 Conditions

All conditions from the Tochnog Order form apply. See our internet page for the latest order form.

2 Validation calculations

Data files are enclosed with the TOCHNOG distribution. These files have several purposes. First, they show the analysis capabilities of TOCHNOG. Second, these input files enable an easy start in performing calculations yourself. Third, the data items **target_item** and **target_value** are used in the data part, allowing you to test TOCHNOG on your specific computer system. This manual only contains results with some of the input files. The files belonging to the validations 1, 2, ... show here are named validation1.dat, validation2.dat, ...

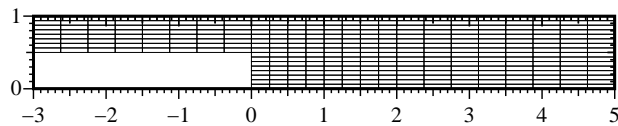
2.1 Validation 1: Backward facing step (fluid flow)

The following specific case of the GAMM workshop [3] is studied here:

total length of channel $L = 22$.
length inflow section $l = 3$.
total height $H = 1$.
height inflow section $h = 0.5$.
viscosity $\nu = 0.01$.
density $\rho = 1$.
maximum flow component of parabolic profile in inflow section $U_{max} = 1$.
the flow volume is $(2/3)hU_{max} = 1/3$.
Reynolds $Re = U_{max}(H - h)/\nu = 50$.

The result for the minimum x-velocity v_x at distance $x = 0.8$ behind the step is studied. This result checks the correct modeling of the recirculation zone after the step. At the distance $x = 0.8$ we find the minimum velocity is $v_x = -0.041$. This happens at $y = 0.1$ above the lower edge. The results of the GAMM workshop were in between -0.066 and -0.018 .

mesh at time_total=0



2.2 Validation 2: Confined compression of fluid filled porous material

In this 1D validation, a porous solid saturated with fluid is compressed by a force F on the solid phase. The length of the test specimen is L , plane strain conditions hold, the Young's modulus is E , Poisson's ratio is ν , permeability k_p , width of test specimen W , thickness T , area $A = WT$. Some non-dimensional variables are introduced

$$X = x/L \quad T = \frac{Hk_p}{L^2}t \quad P = \frac{Ap}{F}$$

$$H = \frac{E(1-\nu)}{(1+\nu)(1-2\nu)}$$

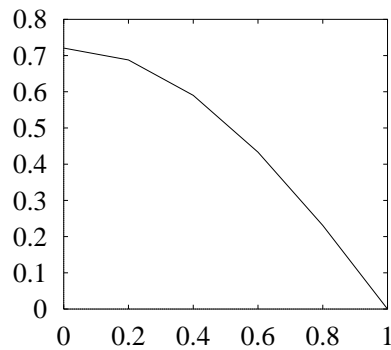
At $X = 1$ free drainage holds ($P = 0$) for $T > 0$. At $X = 0$ the boundary is not permeable ($\frac{\partial P}{\partial X} = 0$) for $T > 0$. Using the non-dimensional variables, the analytical solution reads (see [1])

$$P = \sum_{n=0}^{\infty} \frac{2}{M} \sin(MX) \exp(-M^2T)$$

$$M = \frac{\pi}{2}(2n + 1)$$

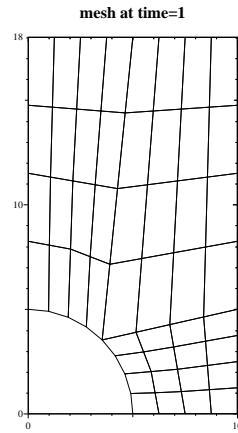
As a typical result, P at $T = 0.22$ is checked; at $X = 0.4$ the exact solution for the non-dimensional pressure P is 0.6.

Now we choose: $L = 1$, $W = 1$, $T = 1$, $E = 1.e1$, $\nu = 0$, $k_p = 0.1$ and $F = 1$. Thus, for $x = 0.4$ at $t = 0.22$ we should find $p = 0.6$. The pressure distribution at $T = 0.22$ is given below



2.3 Validation 3: Plasticity in plate with circular hole

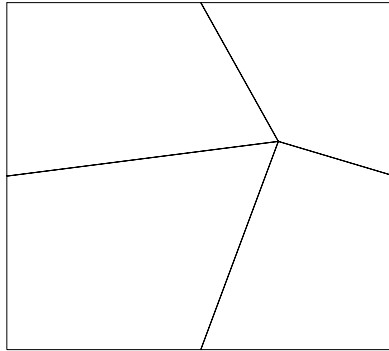
This validation is taken from [5] (page 245). A plate (20 mm wide, 36 mm long) is perforated at the center with a hole with radius 5 mm. The plate is stretched in length direction by increasing the overall strain ϵ in time. The other two boundaries are free to deform. Because of symmetry, only a quarter needs to be modeled. A mesh with 48 linear quadrilateral elements is used



The Young's modulus $E = 7000 \frac{kg}{mm^2}$, Poisson's ratio $\nu = 0.2$, the Von Mises yield stress $\sigma_y = 24.3 \frac{kg}{mm^2}$ and the strain hardening $h = 0.032E = 224 \frac{kg}{mm^2}$. Plane stress conditions hold. The plasticity influence is characterized by σ^{mean} at the upper edge for $v = 0.0625$. The elasto-plastic analysis gives $\sigma^{\text{mean}} = 12.4 \frac{kg}{mm^2}$ for $v = 0.0625$. A purely elastic calculation would have given $\sigma^{\text{mean}} = 16.13 \frac{kg}{mm^2}$.

2.4 Validation 4: Two-dimensional convection and diffusion

This validation demonstrates the effect of the spatial stabilization algorithm in 2D. A convection and diffusion of heat equation is analyzed on a 1 by 1 square. The two-dimensional mesh consists of distorted linear quadrilaterals



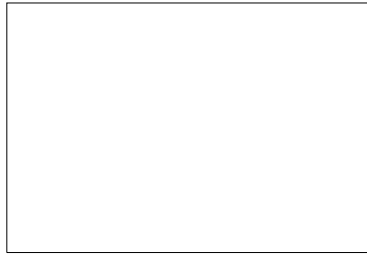
The convection velocity $\beta = 1$ and the conductivity $k = 0.01$. The boundary conditions for temperature are chosen such that the exact solution for a boundary layer in y -direction holds:

$$T(y) = T(y = 0) + (T(y = 1) - T(y = 0)) \frac{1 - \exp(\beta \frac{y}{k})}{1 - \exp(\frac{\beta}{k})}$$

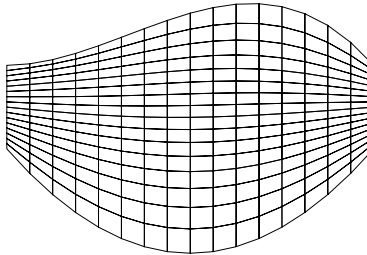
where we choose $T(y = 0) = 1$ and $T(y = 1) = 0$. This is a severe test for the spatial stabilization algorithm. Many algorithms exist which solve this validation exactly when using a one-dimensional domain, say with y -axis only, but few exist which do not show wiggles for irregular 2D grids. The **node_dof** records are initialized with temperature 1 as a first estimate for the solution field. The we check the results at $x = 0.7$ and $y = 0.6$. The exact solution is 1. The numerical solution with the 4-noded elements is 0.95. Splitting the elements in triangles (see **control_mesh_split**) would have given the solution 1.001. Triangles seem to behave better than distorted quads (in this validation anyway). Both solutions are quite good however.

2.5 Validation 7: Global mesh refinement over polynomial domain

This validation shows that mesh refinement follows the boundaries of a domain; more precisely, if the nodes of an element edge are all placed on a specific geometrical entity (**geometry_line**, **geometry_circle**, etc.) then new generated nodes along that edge will also be placed on that geometrical entity; see **refine_globally_geometry** for this. Here we mesh a domain bounded at the left and right side by vertical lines ($x = 0$ and $x = 10$), bounded at the bottom by the polynomial $y = -10 - 10x + x^2$ and bounded at the top by the polynomial $y = +10 + x^2 - 0.1x^3$. Initially only one 4-noded quadrilateral is used



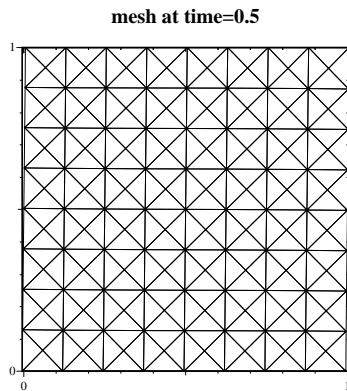
The four nodes of the element are placed on the intersection points of the polynomials and the lines. After 4 global refinements the mesh looks like



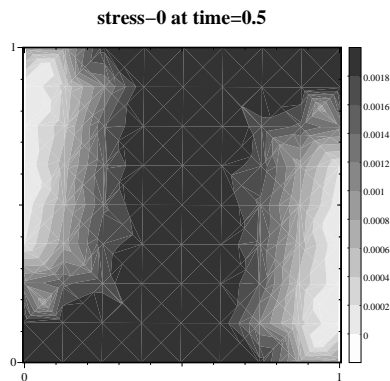
Each refinement is accompanied by some remeshing in order to obtain a more regular mesh.

2.6 Validation 10: Shear of low-tension material (cracking)

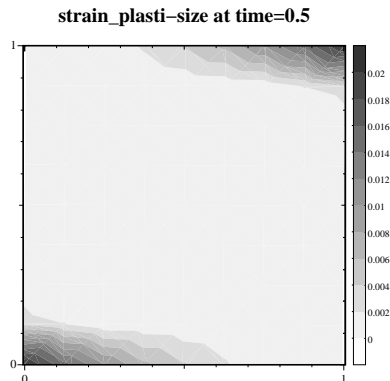
The top edge of a 1 by 1 plate is sheared over 0.01 to the right, and the bottom edge of the plate is sheared over a distance 0.01 to the left. The material cannot sustain positive principal stress exceeding 0.002 — it cracks. This cracking is modeled with a plasticity model which does not allow for principal stresses exceeding 0.002; the `group_materi_plasti_tension` model is used for this. The plate is modeled with linear triangles (`-tria3`). The first plot below shows the (deformed) mesh.



The second plot below shows the largest positive principal stress; notice that this principal stress did become equal to 0.002 over the entire tension diagonal.

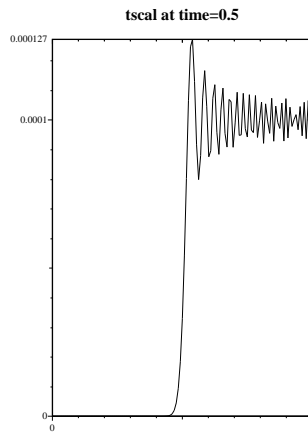


The third plot below shows the plastic strain; plastic strain does show up especially in the corners of the tension diagonal.

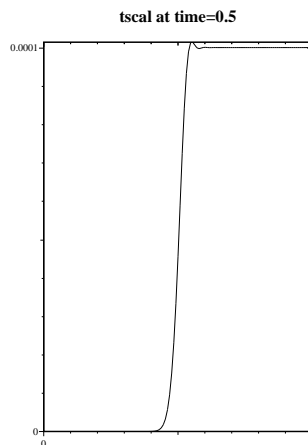


2.7 Validation 11: Propagation of a disturbance in the wave equation.

The wave equation is used over a one-dimensional domain (between $x = 0$ and $x = 1$). The domain is divided into 128 linear elements. At time $t = 0$, $s = 0$ over the entire domain. After time $t = 0$, at $x = 0$ the scalar s is prescribed to hold the value 0 and at $x = 1$ the rate of the scalar s (\dot{s}) is prescribed to have the value $1 \cdot 10^{-4}$. This disturbance at the right edge propagates into the domain with the speed of sound ($c = 1$). At time 0.5 the rate of s over the entire domain is monitored; at this time point \dot{s} should have become $1 \cdot 10^{-4}$ in the right half of the domain, whereas nothing should have happened yet in the left half of the domain. The first plot shows \dot{s} if we use purely explicit time stepping (`control_timestep_iterations` is set to 1).

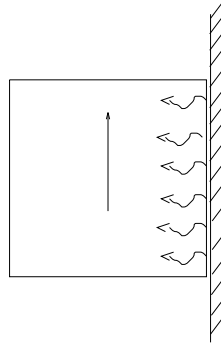


It is clear that the disturbance did propagate into half of the domain, but quite some oscillations do show up. The oscillations are greatly reduced if two iterations are used (`control_timestep_iterations` is set to 2); see the second plot.

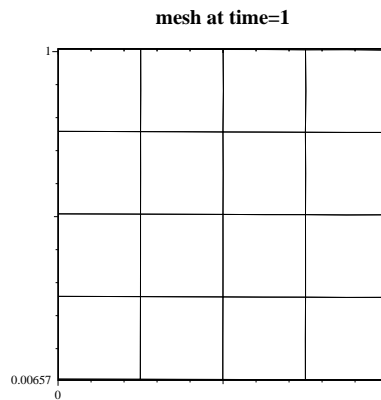


2.8 Validation 12: Contact frictional heat generation.

A rectangular piece of material (size 1 by 1; Young's modulus 1) is rubbed against a solid wall. In this validation, we will analyze the stresses and temperature profile caused by frictional heat generation. The free edges of the material are prescribed to have temperature 0.



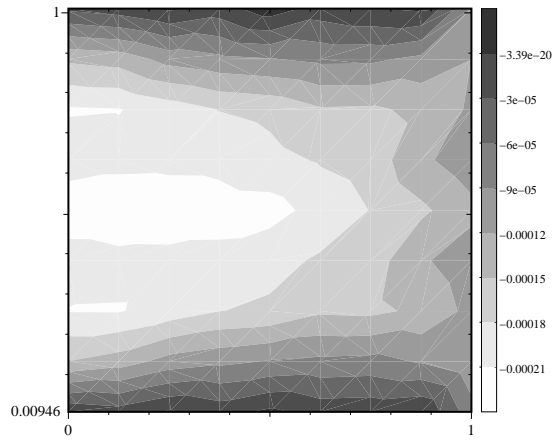
The deformed mesh (with 16 quadratic elements) at time 1 looks like:



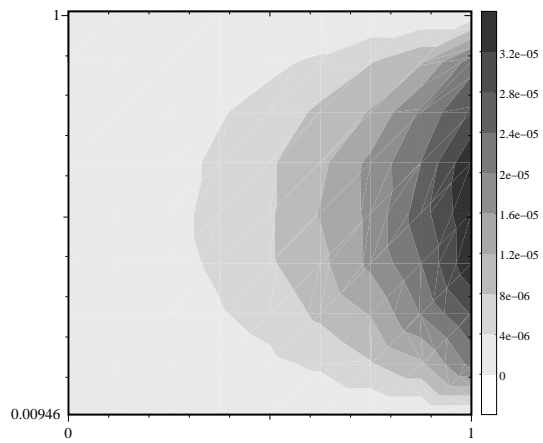
Initially the right edge of the material did penetrate the solid wall over a distance 0.01, but the contact algorithm did eliminate this penetration. This resulted in a normal stress $-\mathbf{sig}_{xx}$ of about size -0.01 . The normal stress causes a frictional stress $-\mathbf{sig}_{xy}$ of about size -0.0001 at the interface between material and solid wall, due to a friction coefficient of 0.01:

This frictional stress, in turn, causes frictional heat generation. The stationary temperature profile is plotted below:

sigxy at time_current=10



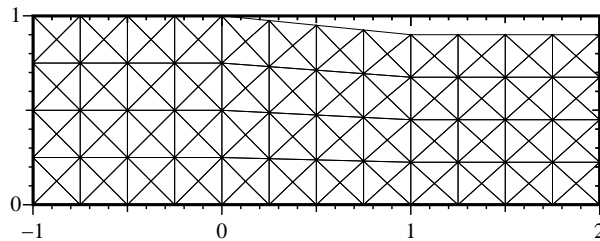
temp at time_current=10



2.9 Validation 14: Continuous metal forming.

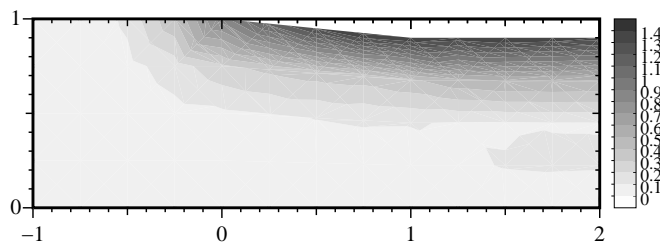
A metal sheet is extruded in a continuous process. The initial thickness of the metal is 1, and the thickness after extrusion is 0.9. The Young's modulus is 7000 and the Poisson ratio is 0.2. The Von Mises plasticity model is used to model permanent deformations (yield stress 24.3). The first flow shows the finite elements mesh:

mesh at time_current=0



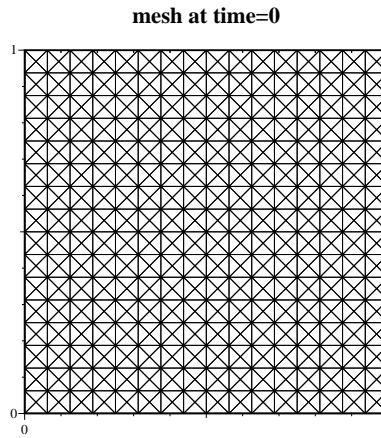
The extrusion is modeled by prescribing a velocity 1.0 at the right edge of the computational domain. On the left edge, the stresses and plastic strains are set to zero, in order to specify that virgin material enters the domain. Friction at the upper wall is not taking into account in this validation. The result for κ , measuring the build up of plastic strains, is plotted below

kap at time_current=5

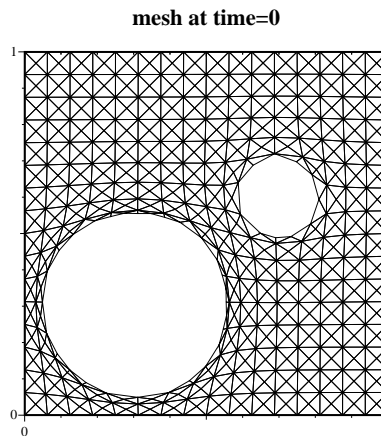


2.10 Validation 15: Generation of two holes in 2D mesh.

This validation demonstrates some mesh manipulation. We start with one 4-noded quadrilateral element (of size 1 by 1). After four global refinements of the mesh, and splitting the 4-noded elements into 3-noded triangles the following mesh is obtained:



Finally a two circular holes are taken out of the mesh, and 10 remeshing passes are applied to get more nicely shaped elements

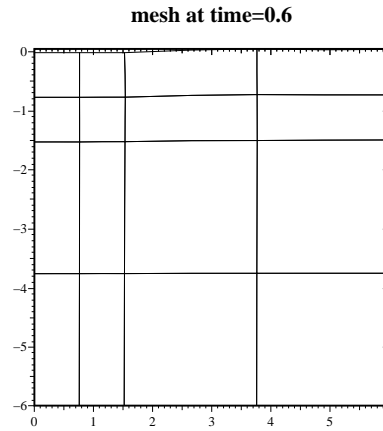


2.11 Validation 16: Bearing capacity of foundation.

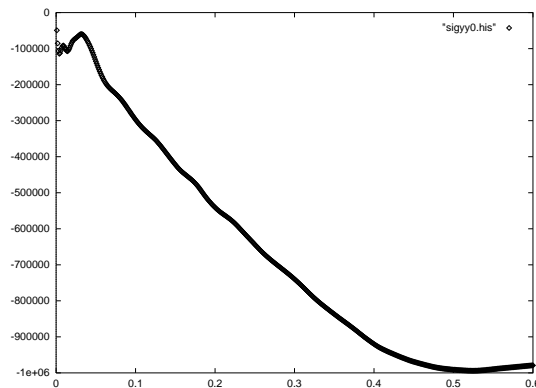
In this plane-strain validation the Mohr-Coulomb plasticity law is used to calculate the bearing capacity of a foundation. The foundation is symmetric, so that only half of the problem is analyzed. The width of (half of) the foundation is 1.52m. The size of the soil domain is taken to be 6m by 6m. The Young's modulus of the soil is $207 \times 10^6 \text{Nm}^{-2}$ and the Poisson ratio is 0.3. For the Mohr-Coulomb law, both the yield rule angle is 20 degrees, and the cohesion is $0.069 \cdot 10^6 \text{Nm}^{-2}$. At the bottom of the domain, all displacements are assumed to be fixed. At the left edge (the symmetry axis) and at the right edge, the horizontal displacement is fixed while the vertical displacement is free.

The classical solutions from Prandtl, Coulomb and Terzaghi give for the maximal average pressure σ_{yy} at the foundation values in the range $0.98 \cdot 10^6 \text{Nm}^{-2}$ up to $1.20 \cdot 10^6 \text{Nm}^{-2}$.

To get the same order of accuracy as in the classical solutions, a coarse mesh with 64 quadratic elements is used. The foundation is prescribed a downward velocity of $0.05 \frac{\text{m}}{\text{s}}$ in the calculation. With time steps of 10^{-3} s the solution is advanced up to time 0.6s. First the deformed mesh at time 1s is plotted below.



Secondly, the development for the average pressure at footing over time is plotted

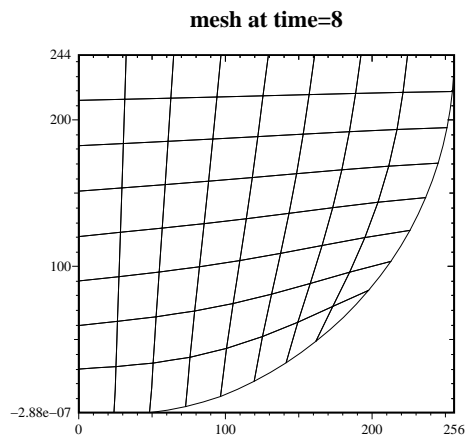


The maximum value of average pressure is near $1.1 \cdot 10^6 \text{Nm}^{-2}$.

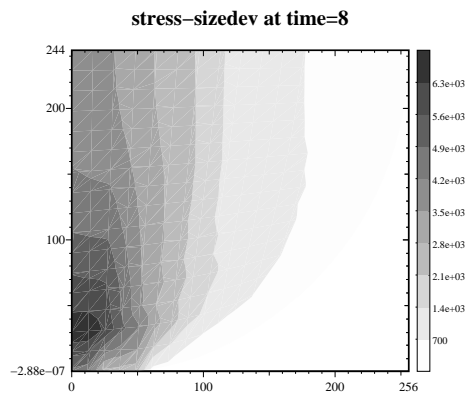
2.12 Validation 17: Hertz contact problem.

A circular solid is compressed to a rigid surface. Due to symmetry only half of the circle needs to be analyzed. The compression is imposed, by prescribing the displacement of the middle line of the circle, so that in fact only one quarter of the circle needs to be analyzed. Plane strain conditions are assumed. The circle radius is 254 mm, the prescribed displacement of the middle line is 10.16 mm, the Young's modulus is 206000 Nmm^{-2} and the Poisson ratio is 0.3. The mesh contains 64 quadratic **-quad9** elements.

The first plot shows the deformed mesh. Notice that the nodes at the bottom of the circle did not penetrate the line $y = 0$.

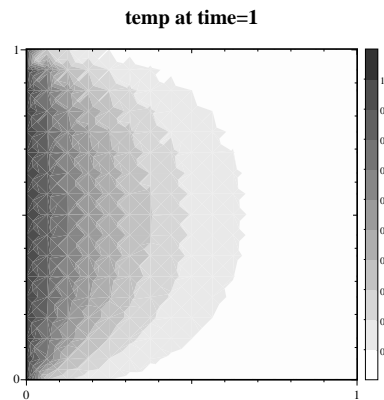


The second plot shows the Mises stresses (the size of the deviatoric stress matrix) in Nmm^{-2} .

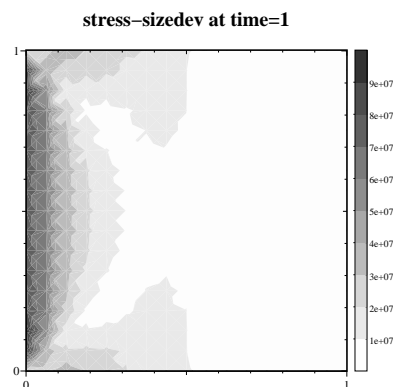


2.13 Validation 18: Thermally induced stresses in plate.

A plate (of size 1 by 1) is initially stress free and in thermal equilibrium with its environment (all initial temperatures are 0). Then the left edge of the plate is prescribed a temperature 1 which will heat the plate. The plate starts convecting energy at its other edges; the coefficient for heat convection is 10^3 , the convection environmental temperature is 0 and the conductivity of the plate is 50. The first plot shows the stationary temperature distribution. A mesh with 16 by 16 linear finite elements is used for the numerical analysis.



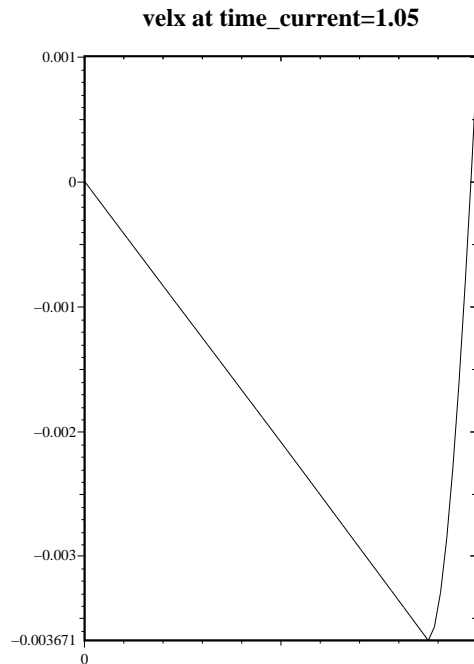
Due to the temperatures, thermal stresses will be induced in the plate. The plate cannot deform at its left edge, but is otherwise free to deform. The Young's modulus is $206 \cdot 10^9$, the Poisson ratio is 0.3, and a plane stress situation is assumed (σ_{zz} is 0). The thermal expansion coefficient is $8.4 \cdot 10^{-4}$. The second plot shows the size of the deviatoric stresses (the von Mises stress) which indicates if plasticity is to be expected.



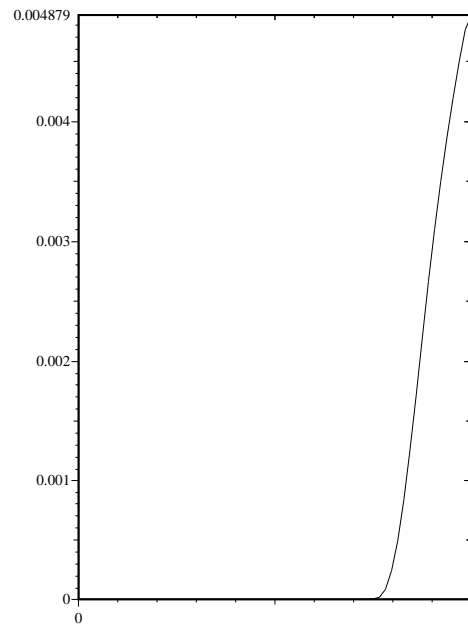
2.14 Validation 19: Nonlocal plasticity in softening bar.

A bar is clamped at the left edge and is subjected at the right edge to a prescribed deformation. A plasticity model is used to limit the possible tensile stress in the bar. This limit of the tensile stress is softened to zero with the effective plastic strain κ . Due to softening, unlimited localization would be possible. This is prevented, however, by applying a viscoplastic power law in combination with a nonlocal yield rule, see **nonlocal** in the users manual. A nonlocal radius of 0.2 is used in the determination of the nonlocal yield rule.

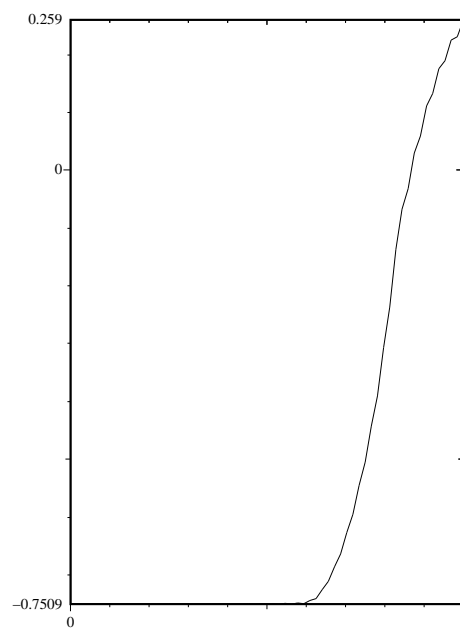
At the right side of the bar we introduce a relatively weak spot, so that plasticity occurs first there. In the plots below the results for the velocity field v_x , the effective plastic strain κ and the nonlocal yield rule f_n respectively are shown. Please notice that the softening zone is of a limited, non mesh dependent, size.



kap at time_current=1.05



fn at time_current=1.05



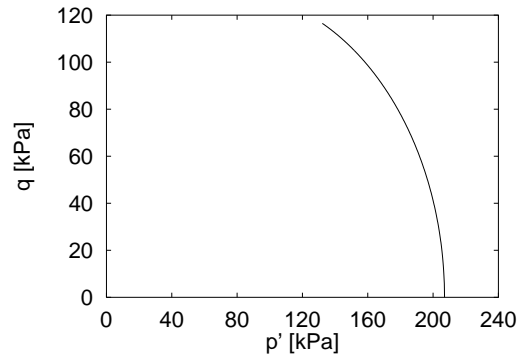
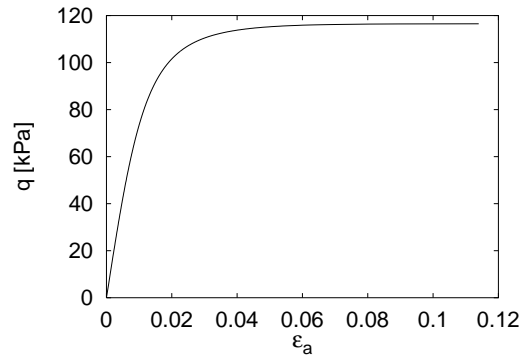
2.15 Validation 22: Constant volume cylindrical compression with Cam Clay.

In soil mechanics, a constant volume cylindrical compression represents the so-called undrained triaxial test. The calculation was performed using a single -quad4 element under axisymmetric conditions. Only small deformations were considered. The parameters of the Cam Clay model correspond to the Weald clay according to [2]: $M = 0.882$, $\lambda = 0.088$, $\kappa = 0.031$, $G = 3000$ kN/m². Initial (effective) stress was isotropic with the mean stress $p' = 207$ kN/m². The void ratio $e = 0.627$ remained constant during the compression due to the imposed constant volume condition. The initial preconsolidation mean pressure was $p_0 = 207$ kN/m².

The calculated stress-strain curve (q is the stress deviator and ε_a is the compressive axial deformation) in the left figure corresponds exactly to the numerically integrated equations of the model. The stress path in the right figure coincides with the analytical solution, see [4]:

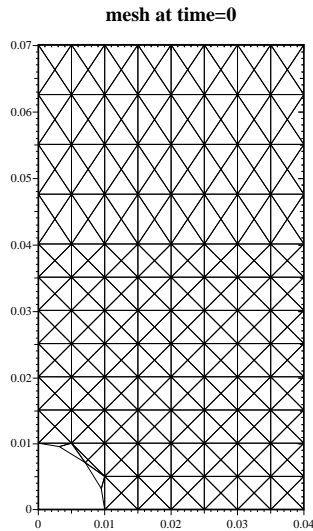
$$\frac{p'_i}{p'} = \left(\frac{M^2 + \eta^2}{M^2 + \eta_i^2} \right)^\Lambda$$

where $\eta = q/p'$ and $\Lambda = (\lambda - \kappa)/\lambda$. The subscript i denotes initial values.

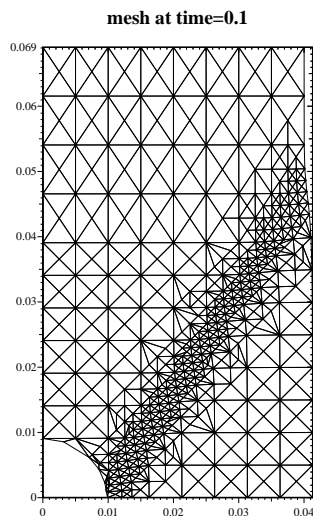


2.16 Validation 23: Automatic local mesh refinement near shear band.

A test specimen is subjected to a vertical compression. The initial mesh is given in the first plot



A hole is present in the down left corner; this hole triggers a shear band. Symmetry boundary conditions are applied, so that in fact the quarter part of a total test specimen is modeled. After the test specimen is compressed, automatic local mesh refinement is applied; the elements with the highest plastic strains are refined. Then the calculation restarts with the new mesh automatically. This refinement + automatic restart is done three times. The final plot shows the deformed mesh after the three refinements.



References

- [1] H.S. Carslaw, J.C. Jeager 1974 *Conduction of heat in solids* Clarendon Press Oxford
- [2] Carter, J.P., 1982. Predictions of the non-homogeneous behaviour of clay in the triaxial test. *Géotechnique*, Vol. 32, No. 1, 55-58.

- [3] K. Morgan, J. Periaux, F. Thomasset *1984 Analysis of Laminar Flow over a Backward Facing Step* Notes on Numerical Fluid Mechanics, a GAMM-workshop Friedr. Vieweg & Sohn Braunschweig/Wiesbaden
- [4] Wood, D.M., 1990. Soil behaviour and critical state soil mechanics. Cambridge University Press.
- [5] O.C. Zienkiewicz, R.L. Taylor *The finite element method Volume2, fourth edition* McGraw-Hill Book Company London